David Tomás Sánchez Martínez
Lourdes García Rodríguez
(coordinadores)

Proceedings of the 7th International Seminar on ORC Power Systems

Editorial Universidad de Sevilla

Proceedings of the 7th International Seminar on

ORC
Power Systems

David Tomás Sánchez Martínez
Lourdes García Rodríguez
(coordinadores)

Proceedings of the 7th International Seminar on

ORC Power Systems

(ORC2023)

4th to 6th
SEPTEMBER
SEVILLE 2023

EDITORIAL UNIVERSIDAD DE SEVILLA

Sevilla, 2024

Colección Actas
Núm.: 91

Review chairs of the 7th International Seminar on ORC Power Systems

Prof. Christoph Wieland (University of Duisburg-Essen) - *Review Chair*
Prof. Sotirios Karellas (National Technical University of Athens) - *Review Co-Chair*
Prof. Teemu Turunen-Saaresti (LUT University) - *Review Co-Chair*
Dr. Diego-César Alarcón-Padilla (Plataforma Solar de Almería - CIEMAT) - *Review Co-Chair*
Dr. Francesco Crespi (Universidad de Sevilla) - *Review Co-Chair*

ISBN 978-84-472-2745-7
DOI: https://dx.doi.org/10.12795/9788447227457

Diseño de cubierta y maquetación: los autores

INDEX OF CONTRIBUTIONS

ID3 - Additive manufacturing for fast prototyping of a velocity compounded radial re-entry turbine
Authors: Dominik Stümpfl, Karel Ráž, Philipp Streit, Andreas P. Weiß 13

ID4 - Thermodynamic concept of a novel recuperative two-phase power cycle process
Authors: Benedikt G. Bederna, Riley B. Barta, Christiane S. Thomas. 23

ID7 - Performance analysis of a 1.5 MW Organic Rankine Cycle in a Carnot battery system for grid balancing services
Authors: Robin Tassenoy, Hannes Van De Velde, Kenny Couvreur, Michel De Paepe, Steven Lecompte 33

ID8 - Calibration of multi-hole probes for measurements in compressible organic vapor flows
Authors: Leander Hake, Stephan Sundermeier, Stefan Aus Der Wiesche, Maximilian Passmann 43

ID9 - pocketORC: A browser-based calculator for teaching organic Rankine cycle power systems
Authors: Martin White 53

ID10 - Evaluation of existing supercritical heat transfer correlations for designing the vapor generator in low-temperature transcritical Organic Rankine Cycle systems
Authors: Jera Van Nieuwenhuyse, Anastasios Skiadopoulos, Dimitris Manolakos, Steven Lecompte, Michel De Paepe 61

ID12 - A novel combined cooling and power cycle integrated ejector refrigeration and composition adjustment for stationary engine waste heat recovery
Authors: Xiaocun Sun, Lingfeng Shi, Hua Tian, Gequn Shu 71

ID14 - Design and construction of a reversible ORC test rig for geothermal CHP applications
Authors: Florian Kaufmann, Christopher Schifflechner, Christoph Wieland, Hartmut Spliethoff 81

ID15 - Robust and fast meanline methodology for radial inflow turbines with non-ideal gases for system level optimisation of organic Rankine cycles
Authors: Carola Freytag, Eva Alvarez-Regueiro, Pablo Ale-Martos, Esperanza Barrera-Medrano, Ricardo Martinez-Botas. 91

ID16 - Shape optimization of a sCO2 centrifugal compressor stage
Authors: Alessandro Romei, Paolo Gaetani, Giacomo Persico 101

ID17 - Optimizing the performance of a hybrid solar-biomass micro-CHP system with a TFC engine as the prime mover for domestic applications
Authors: Anastasios Skiadopoulos, Xander Van Heule, Steven Lecompte, Michel De Paepe, Dimitrios Manolakos 109

ID19 – Systematic and multi-criteria optimisation of subcritical thermally integrated Carnot batteries (TI-PTES) in an extended domain
Authors: Antoine Laterre, Olivier Dumont, Vincent Lemort, Francesco Contino 119

ID20 - ORC technology used in a heat removal system for an advanced nuclear power plant
Authors: Guillaume Lhermet, Benoit Payebien, Nicolas Tauveron, Nadia Caney, Franck Morin . . . 130

ID22 - Assessment of trilateral Organic Rankine Cycle for solar applications with innovative turboexpander concept
Authors: Alessandro Romei, Andrea Giostri, Andrea Spinelli . . . 140

ID25 - Evaluation of the performance of an axial one-stage 10kW turbogenerator through experimental testing
Authors: Piotr Klimaszewski, Piotr Klonowicz, Lukasz Witanowski, Tomasz Suchocki, Piotr Lampart, Eugeniusz Ihnatowicz, Lukasz Antczak, Dawid Zaniewski, Lukasz Jedrzejewski . . . 149

ID26 - Investigation of the turbulence level and the vortex shedding in a turbine cascade working with an organic vapor at subsonic Mach numbers
Authors: Leander Hake, Stephan Sundermeier, Stefan Aus Der Wiesche, Camille Matar, Paola Cinnella, Xavier Gloerfelt . . . 159

ID27 - A novel approach to district heating: using a two-phase expander in a reversible heat pump-Organic Rankine Cycle system
Authors: Sindu Daniarta, Attila R. Imre, Piotr Kolasinski . . . 169

ID28 - Optimization of a partially evaporating Organic Rankine Cycle with thermal non-equilibrium expansion
Authors: Xander Van Heule, Tasos Skiadopoulos, Dimitris Manolakos, Michel De Paepe, Steven Lecompte . . . 176

ID29 - Cost-effective option of cold energy utilization in pharmaceutical industry
Authors: Sindu Daniarta, Dawid Sowa, Ádám Havas, Attila R. Imre, Piotr Kolasinski . . . 184

ID30 - Numerical investigation of a transonic dense gas flow over an idealized blade vane configuration
Authors: Aurelien Bienner, Xavier Gloerfelt, Paola Cinnella, Leander Hake, Stefan Aus Der Wiesche . . . 193

ID31 - Comprehensive analysis of ORC-VCC system for air conditioning from low-temperature waste heat
Authors: Lukasz Witanowski . . . 203

ID33 - Pareto front analysis for the design and the working fluid selection in ORC-based pumped thermal energy storage technology in both pure electric and cogenerative applications
Authors: Marco Astolfi, Dario Alfani, Andrea Giostri . . . 214

ID36 - Evaluating the waste heat sources in a very large crude carrier and the potential integration of Organic Rankine Cycle configurations
Authors: Amalia Stainchaouer, Christopher Schifflechner, Christoph Wieland, Hartmut Spliethoff . . . 224

ID37 - Investigating R1234ze and R1234yf as replacements to R134a in waste heat recovery ORC applications
Authors: James Bull, James Buick, Jovana Radulovic . . . 234

ID38 - Performance and economic assessment of a thermally integrated reversible HP/ORC Carnot battery applied to data centers
Authors: Chiara Poletto, Andrea De Pascale, Saverio Ottaviano, Olivier Dumont, Maria Alessandra Ancona, Michele Bianchi 244

ID39 - Evaluation of the performance of multiple supercritical CO2 power cycles in Waste Heat Recovery applications
Authors: Hicham Chibli, Matthew Read, Abdulnaser Sayma 254

ID40 - Design and modeling of a demonstration-scale ORC cycle for the Liquid Air Combined Cycle
Authors: Owen Pryor, William Conlon, Aaron Rimpel, Milton Venetos 264

ID41 - Guidelines and optimization criteria of a machine learning-based methodology for mixture design in ORC systems
Authors: Valerio Mariani, Saverio Ottaviano, Andrea De Pascale, Giulio Cazzoli, Lisa Branchini, Gian Marco Bianchi 273

ID45 - Potential of trigenerative Waste Heat Recovery CO2-mixture transcritical power plants for increasing the sustainability of district heating and cooling networks
Authors: Mattia Baiguini, Michele Doninelli, Ettore Morosini, Dario Alfani, Gioele Di Marcoberardino, Paolo Giulio Iora, GiampaoloManzolini, Constante Mario Invernizzi, Marco Astolfi 282

ID46 - Thermodynamic analysis of a novel pumped thermal energy storage system with waste heat integration
Authors: Meiyan Zhang, Lingfeng Shi, Peng Hu, Gang Pei, Gequn Shu 294

ID48 - Pressure profile optimisation of a nozzle for wet-to-dry expansion
Authors: Pawel Ogrodniczak, Abdulnaser Sayma, Martin T. White 304

ID51 - Thermodynamic modification of CO2-based combined cooling and power cycle with ejector
Authors: Yonghao Zhang, Lingfeng Shi, Gequn Shu 313

ID53 - Selection of suitable working fluid and storage material for ORC coupled with Thermal Energy Storage
Authors: Dawid Sowa, Sindu Daniarta, Piotr Kolasinski 323

ID54 - Influence of dopant fluorination on the heat transfer behaviour of CO2-based mixtures in transcritical power cycles
Authors: Michele Doninelli, Gioele Di Marcoberardino, Costante Mario Invernizzi, Paolo Giulio Iora 333

ID57 - On air-cooled condensers for ORC systems operating with zeotropic mixtures
Authors: Lorenzo Galieti, Carlo De Servi, Dario Alfani, Paolo Silva, Paola Bombarda, Piero Colonna 344

ID58 - Experiments on supersonic ORC nozzles in linear cascade configuration
Authors: Marco Oliveti, Marco Manfredi, Giacomo Persico, Andrea Spinelli, Paolo Gaetani, Vincenzo Dossena 354

ID59 - Numerical analysis of aerodynamics and performance of a radial-inflow micro-ORC turbine
Authors: Fatemeh Ardaneh, Marta Zocca, Antti Uusitalo, Teemu Turunen-Saaresti. 363

ID61 - ORC system using R1233zd(E) for waste heat recovery from the upstream process
Authors: Meng Soon Chiong, Bemgba Nyakuma, Nur Izwanne Mahyon, Srithar Rajoo, Eva Alvarez-Regueiro, Maria Esperanza Barrera-Medrano, Ricardo F. Martinez-Botas, Yossapong Laoonual 373

ID63 - Experimental investigation of a small-scale reversible high temperature heat pump – Organic Rankine Cycle system for industrial Waste Heat Recovery
Authors: Rahul Velanparambil Ravindran, Donal Cotter, Christopher Wilson, Ming Jun Huang, Neil Hewitt. 381

ID64 - Technical comparison and evaluation of a Pumped Thermal Energy Storage with two different designs
Authors: Márcio Santos, Jorge André, Ricardo Mendes, José Ribeiro. 391

ID68 - The potential of CO2-Plume Geothermal (CPG) Systems for CO2 component manufacturers: opportunities and development needs
Authors: Christopher Schifflechner, Jasper De Reus, Hartmut Spliethoff, Martin O. Saar, Sebastian Schuster, Dieter Brillert 400

ID69 - Development of a generalised low-order model for twin-screw compressors
Authors: Florian Kaufmann, Ludwig Irrgang, Christopher Schifflechner, Hartmut Spliethoff. 410

ID71 - Decision-making matrix for the selection of mixture in ORC applications
Authors: William Combaluzier, Nicolas Tauveron, Michel Beaughon, Aldo Serafino 420

ID72 - Reversible heat pump-ORC pilot plant – Experimental results and fluid charge optimization
Authors: Maximilian Weitzer, Sebastian Kolb, Dominik Müller, Jürgen Karl 430

ID73 - Performance of Organic Rankine Cycle system in combination with residual municipal solid waste gasification: a simulation analysis
Authors: Luca Cioccolanti, Giovanni Biancini, Ramin Moradi, Luca Del Zotto, Matteo Moglie 439

ID74 - Enhancing knowledge of engineering students at all levels on organic rankine cycle systems for their application in the built environment
Authors: Luca Cioccolanti, Ramin Moradi, Ermira Abdullah, Syamimi Saadon, Mohamad Yusof Idroas, Teoh Yew Heng, Kwanchai Kraitong 449

ID75 - Studying carbon dioxide and acetone mixtures in a single-stage absorption-compression cycle for heating and cooling applications
Authors: Jesús Gómez-Hernández, Ali Kholghi, Mercedes De Vega, Javier Villa, Ronan Grimes 458

ID77 - Valorising thermal composite recycling processes using Organic Rankine Cycles for combined heat and power applications
Authors: Ramin Moradi, Liu Yang 466

ID80 – Prediction of the ideal maximum operational temperature of hydrocarbon and HFCs as working fluids of Organic Rankine Cycle power plants based on transition state theory
Authors: Wei Yu, Chao Liu, Xijie Ban, Zhirong Li, Tianlong Yan 476

ID82 - Comparison of different evaporator topologies for industrial heat pumps
Authors: Sanjay Vermani, Nitish Anand, Johan Van Bael, Evgueni Touliankine, Aldo Serafino, Carlo De Servi. 486

ID83 - On the plant improvement of Solar-driven ORC based power unit for domestic microcogeneration
Authors: Fabio Fatigati, Marco Di Bartolomeo, Arianna Coletta, Diego Vittorini, Giammarco Di Giovine, Davide Di Battista, Roberto Cipollone 496

ID84 - Mapping the techno-economic potential of next-generation CSP plants running on transcritical CO2-based power cycles
Authors: Pablo Rodríguez-deArriba, Francesco Crespi, Sara Pace, David Sánchez 505

ID86 - Achieving 45% micro gas turbine efficiency through hybridization with Organic Rankine Cycles
Authors: Antonio Escamilla, David Sánchez Martínez, Lourdes García-Rodríguez 515

ID88 - Operational optimisation of the main heat rejection unit of CSP plants based on carbon dioxide mixtures
Authors: Francesco Crespi, Pablo Rodríguez-deArriba, Lourdes García-Rodríguez, David Sánchez. 525

ID89 - Mechanical design and rotor-dynamic analysis of the ORCHID turbine
Authors: Matteo Majer, Steven Chatterton, Ludovico Dassi, Alessio Secchiaroli, Edoardo Gheller, Carlo De Servi, Paolo Pennacchi, Piero Colonna, Matteo Pini 535

ID91 - Thermodynamic feasibility of a pumped thermal energy storage driven by ocean temperature gradient
Authors: Alessandra Ghilardi, Andrea Baccioli, Guido Francesco Frate, Lorenzo Ferrari 545

ID92 - Exergy-based methods for heat pumps
Authors: Mathias Hofmann, Jonas Freißmann, Malte Fritz, Jeremias H. Alexe, Francesco Witte, George Tsatsaronis 553

ID93 - Reduced order modelling of optimized heat exchangers for maximum mass-specific performance of Airborne ORC Waste Heat Recovery units
Authors: Fabio Beltrame, Dabo Krempus , Piero Colonna, Carlo De Servi. 563

ID97 - Basic design of an ORC demonstrator system for implementation in an Iron & Steel plant through the DECAGONE project
Authors: Magnus Windfeldt, Han Deng, Trond Andresen, Christopher Schifflechner 574

ID98 - Analytical estimation of the presence of non-condensable gases in the condensate tank of an Organic Rankine Cycle
Authors: Radheesh Dhanasegaran, Antti Uusitalo, Juha Honkatukia, Teemu turunen-Saaresti 584

ID101 - Advanced control of compressor inlet temperature in supercritical CO2 Brayton cycle
Authors: Rui Wang, Xuan Wang, Hua Tian, Gequn Shu. 596

ID103 - Potential for surplus-heat-to-power conversion in current and future aluminium production processes with off-gas recycling
Authors: Jonas Bueie, Magnus Windfeldt, Trond Andresen. 605

ID104 - Investigating the application range of ORC power plants for the exploitation of two-phase geothermal resources
Authors: Tristan Merbecks, Claudio Pietra, Paola Bombarda, Martin O. Saar, Paolo Silva, Dario Alfani. 615

ID109 - Cold Energy Recovery in LNG plants with Organic Rankine Cycle
Authors: Gabriele Marchiori, Marta Giudici, Giorgia Ruffato, Marco Astolfi 626

ID110 - Numerical investigation of organic vapor flow effects on a micro-scale radial turbocompressor
Authors: Andrés Sebastián, Rubén Abbas, Manuel Valdés 636

ID112 - Design, modeling and simulation of an experimental Rankine PTES system
Authors: Mario Petrollese, Giorgio Cau, Matteo Marchionni, Marcello Lorenzo Marroccu, Rosa Merchan 645

ID113 - Small-scale turbopumps for Waste Heat Recovery applications based on an Organic Rankine Cycles, modeling, analytical and experimental investigation
Authors: Sajjad Zakeralhoseini, Jürg Schiffmann 655

ID116 - Double-stage ORC system based on various temperature waste heat sources of the negative CO2 power plant
Authors: Kamil Stasiak, Pawel Ziólkowski, Dariusz Mikielewicz 665

ID117 - Optimization of organic Rankine cycle in ocean thermal energy conversion based on NSGA-II
Authors: Zheng Hu, Jiufa Chen, Bing Guo, Chengbin Zhang 679

ID118 - TES4Trig: Development of a demonstrator for the production of electricity, heating and cooling based on an Organic Rankine and an Ejector Cooling Cycle driven by high-temperature parabolic trough collectors with thermal energy storage
Authors: Konstantinos Braimakis, Dimitrios Tziritas, George Stavrakakis, Julio Terrón Gutiérrez, Siddhart Dutta, Christos Xynos, Panagiotis Zervas, Sotirios Karellas 689

ID119 - Simulation and operation of a CSP that works with a HRB Cycle
Authors: Antonio J. Subires, Antonio Rovira 701

ID123 - Towards a green energy community: integration of micro-ORCs combined with renewable energy technologies in buildings
Authors: Diego Antonio Rodríguez Pastor, Víctor Manuel Soltero Sánchez, Elisa Carvajal Trujillo, José Antonio Becerra, Ricardo Chacartegui 713

ID129 - Assessment of high temperature heat pump layouts equipped with a bladeless turboexpander
Authors: Matteo Passalacqua, Simone Maccarini, Stefano Barberis, Alberto Traverso 723

ID133 - Selection of the optimal working fluid in an Organic Rankine Cycle for Waste Heat Recovery through multi-objective optimization and decision making
Authors: Bipul Krishna Saha, El Mouatez Billah Messini, Syed J. Hoque, B Aneesh Bhat, Pramod Kumar 733

ID139 - Dual condensing pressure ORC for cryogenic energy storage
Authors: William M. Conlon, Milton J. Venetos 743

ID141 - Optimum coupling of thermal energy storage and power cycles for Carnot batteries
Authors: Salvatore Guccione, Rafael Guedez 751

ID142 - Aerodynamic design and numerical analysis of a counter-rotating centrifugal compressor
Authors: Cheikh Brahim Abed, Arthur Leroux 761

DOI: https://dx.doi.org/10.12795/9788447227457_117

Optimization of organic Rankine cycle using ocean thermal energy based on NSGA-II

Zheng Hu [1], Jiufa Chen [1,2], Bin Guo [3], Chengbin Zhang [1,*]

[1] *Key Laboratory of Energy Thermal Conversion and Control of Ministry of Education, School of Energy and Environment, Southeast University, Nanjing, Jiangsu 210096, P. R. China*
[2] *Nanjing Purple Mountain Institute Ltd, 6 Fengxin Road, Yuhua District, Nanjing, Jiangsu 210096, P. R. China*
[3] *College of Water Conservancy and Civil Engineering, Shandong Agricultural University, Taian, Shandong 271018, P. R. China*
230198429@seu.edu.cn, chen.jiufa@seu.edu.cn, guobin@sdau.edu.cn, cbzhang@seu.edu.cn,
*Corresponding Author

ABSTRACT

The organic Rankine cycle is one of the key methods to utilize ocean thermal energy, which is abundant and continuous renewable energy. In this paper, a non-dominated sorting genetic algorithm-II (NSGA-II) based approach is utilized to optimize an organic Rankine cycle-based ocean thermal energy conversion system. The objective is to maximize the degree of thermal energy utilization and the maximum system power output in. The decision variables considered for optimization include evaporation temperature, condensation temperature, degree of superheating, and working fluid mass flow. The objective functions are defined as thermal efficiency and net power output. The optimization process for the ocean thermal energy conversion Rankine cycle is performed using NSGA-II. The results indicate an inverse relationship between thermal efficiency and power output, meaning that achieving the highest thermal efficiency does not necessarily result in the highest net power output. The utilization of NSGA-II enables the identification of multiple optimal solutions that lie on the Pareto front, representing the best trade-off between thermal efficiency and power output. By considering the investment cost constraint, the most suitable solution for achieving the maximum net power output can be determined.

1 INTRODUCTION

Ocean thermal energy refers to the thermal energy stored within the temperature gradient between surface warm sea water and deep cold seawater. It owns the advantages of stableness, non-fluctuation with temporal and spatial variance. Closed Organic Rankine Cycle (ORC) is the most promising for commercial application of ocean thermal energy conversion (OTEC) since it has the simplest configuration and is easy to miniaturize. However, ocean thermal energy functions within a small temperature gradient (usually ≤23°C) and has low thermal efficiency (usually around 3%). To improve thermal efficiency, many researchers focus on the selection of working fluids, optimization of cycle configuration. Hung *et al*. (2010) found that at low temperature difference conditions, the working fluids with high latent heat of evaporation can achieve higher thermal efficiency. Ganic *et al*. (1980) compares the performance of a closed ORC cycle using inorganic working fluid (ammonia), and organic working fluids (R290, R114). The results show that using ammonia as working fluid can achieve the highest thermal efficiency since its latent heat of evaporation is the highest. In the OTEC process, the temperature fluctuation of warm sea water inside the evaporator will increase the temperature difference between the working fluid outlet of the evaporator and heat source, causing the irreversible loss of heat transfer when using pure working fluid. Therefore, in recent years, researchers are searching for non-zeotropic working fluid to enhance OTEC's efficiency (Araghi *et al*, 2016; Yoon *et al*, 2015). Meanwhile, methods to improve the ORC cycle, such as the introduction of heat recovery heat exchanger, ejector and multi-stage expansion in the system design, can also enhance the efficiency (Yoon *et al*, 2015).

Both the adoption of non-zeotropic working fluid and the improvement of the ORC cycle add the complexity of the ORC system. Optimizing the design and operation parameters of the ORC cycle can be another solution to enhance the system's performance. Sun *et al*. (2012) selected warm sea water temperature, warm sea water flow rate, evaporation temperature and condensation temperature as decision variables, and ORC net power generation as target variables. The optimal system design parameter is obtained. Wang *et al*. (2019) set evaporation temperature, condensation temperature, warm seawater outlet temperature and cold sea water outlet temperature as optimization variables, and levelized electricity cost and exergy efficiency as objective functions. The normalized Pareto front was obtained using multi-objective particle swarm optimization algorithm. In summary, most researches work on OTEC performance enhancement focus on the selection of working fluids and cycle improvement, while research focusing on optimization of the design and operation parameter are less and only limited to single objective optimization.

To deepen the understanding of the thermal characteristics of OTEC based on closed ORC, this paper established the theoretical static model for the closed ORC cycle. The impact of evaporation temperature, condensation temperature, superheat at turbine inlet and flow rate on the turbine output, cycle thermal efficiency, system investment cost and levelized cost of electricity are calculated and analyzed. Based on this, the generic algorithm is adopted to conduct bi-objective optimization based on the OTEC power plant. In the design optimization, the turbine output power and thermal efficiency are the objective functions, the system investment cost, warm and cold seawater flow rate are the constraints, the evaporation temperature, condensation temperature, turbine inlet overheat and flow rate of working fluids are the optimization variables. Non-dominated Sorting Generic Algorithm is adopted to conduct bi-objective optimization of OTEC and obtain Pareto front of the turbine output power and thermal efficiency to guarantee the maximum thermal efficiency under the designed installed capacity of OTEC.

In summary, this paper demonstrates the use of NSGA-II for optimizing an organic Rankine cycle-based ocean thermal energy conversion system. The methodology considers multiple decision variables 680
and objectives, leading to a set of Pareto-optimal solutions. The study highlights the trade-off between thermal efficiency and power output and provides valuable insights for selecting the optimal design that maximizes net power output within the specified investment cost constraint.

2 OTEC MODEL

2.1 System description

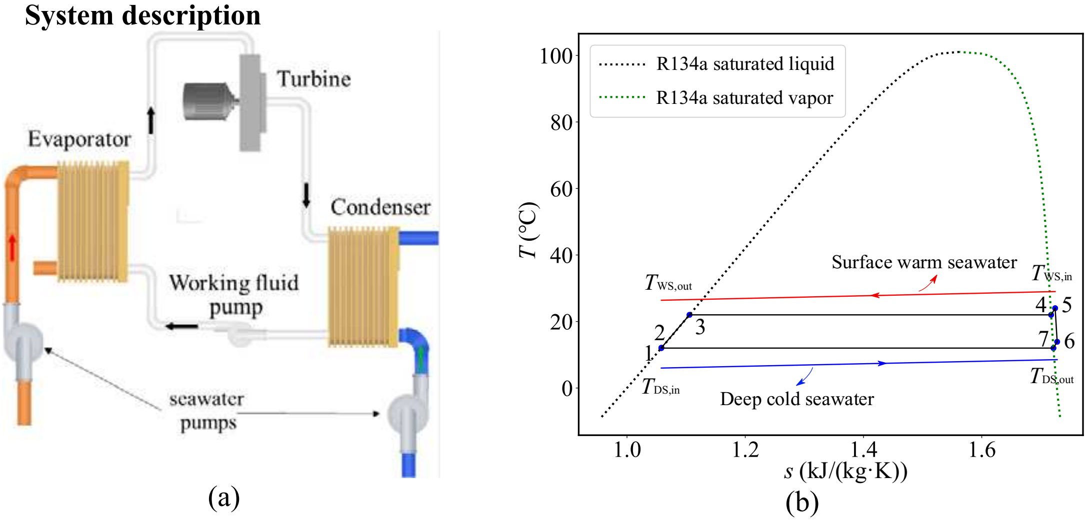

Figure 1: Rankine cycle-based OTEC: (a) working principle, (b) *T-s* diagram.

OTEC system utilizes the temperature gradient between warm surface seawater and cold deep seawater to generate electricity. Figure 1 provides the schematic of Rankine cycle-based OTEC.

Organic fluid R134a is selected as the working fluid. Liquid R134a (state point 1) is pressurized to state point 2 and sent into the evaporator. The working fluid exchange heat with warm surface seawater in the evaporator, which goes through saturated liquid state (point 3), saturated gas state (point 4) and overheat state (point 5). The gas-phase working fluid enters turbine at the evaporator outlet for expansion to generate electricity, while the exhaust gas at the turbine outlet (state point 6) enters the condenser for heat exchange and condenses to state point 1.

2.2 Thermodynamic model

The key to the thermodynamic calculation is to determine the thermodynamic parameters at each point on the *T-s* diagram. Therefore, the thermodynamic model of the cycle is established in Matlab according to the conservation of energy and mass, and the other thermodynamic parameters (including enthalpy and entropy) at each state point are determined by the pressure and temperature parameters, and the physical properties of the work material are calculated using Refprop. The energy equations for each component are listed in Table 1.

Table 1: Energy equations for ORC-based OTEC system

Components	Equations
Working fluid pump	$W_{\text{pump,wf}} = m_{\text{wf}}(h_1 - h_2) = m_{\text{wf}}(h_1 - h_{2,\text{is}})\eta_{\text{pump,wf}}$
Evaporator	$m_{\text{WS}} \cdot c_{\text{p,WS}} \cdot (T_{\text{WS,in}} - T_{\text{WS,out}}) = m_{\text{wf}}(h_5 - h_2)$
Turbine	$W_{\text{tur}} = m_{\text{wf}}(h_5 - h_6) = m_{\text{wf}}(h_5 - h_{6,\text{is}})\eta_{\text{tur}}$
Condenser	$m_{\text{DS}} \cdot c_{\text{p,DS}} \cdot (T_{\text{DS,in}} - T_{\text{DS,out}}) = m_{\text{wf}}(h_6 - h_1)$
Seawater pumps	$W_{\text{pump,SW}} = \dfrac{Qv_{\text{SW}}\Delta P_{\text{t}}}{\eta_{\text{pump,SW}}}$
The subscript pump stands for pump, wf stands for working fluid, η stands for isentropic efficiency of pump; eva and con refer to evaporator and condenser, respectively, WS and DS refer to warm seawater and deep seawater, tur stands for turbine, η_{tur} stands for turbine isentropic expansion efficiency of the turbine, Q_v stands for volume flow rate, ΔP_t is the total pressure loss during seawater transportation which can be calculated according to Hu *et al.* (2022).	

Hence, the Net power generation of ORC is obtained by

$$W_{\text{net}} = W_{tur} - W_{\text{pump,wf}} - W_{\text{pump,WS}} - W_{\text{pump,DS}} \tag{1}$$

The net thermal efficiency is given by

$$\eta_{\text{themal}} = \frac{W_{\text{net}}}{Q_{\text{eva}}} \tag{2}$$

The heat transfer areas of the evaporator and condenser can be calculated by

$$Q = UA\Delta T \tag{3}$$

where, U is total heat transfer coefficient, A is the total heat transfer area, ΔT is Logarithmic mean temperature difference (LMTD).

The total heat transfer coefficient is calculated by

$$\frac{1}{U} = \frac{1}{h_{\text{h}}} + \frac{\delta}{\lambda_{\text{p}}} + \frac{1}{h_{\text{c}}} + R_{\text{f}} \tag{4}$$

where, h_h and h_c are the convective heat transfer coefficient on hot and cold sides, respectively, δ is the plate thickness, λp is the thermal conductivity of the plate, R_f is the thermal resistance of dirt.

The LMTD is calculated by

$$\Delta T = \frac{\Delta T_{\text{max}} - \Delta T_{\text{min}}}{\ln(\Delta T_{\text{max}}/\Delta T_{\text{min}})} \tag{5}$$

For the evaporator, only a single-phase heat transfer model is established for the warm sea water side. For working fluid in the evaporator, since it goes through subcooling, evaporation and overheat processes. The subcooling and superheat processes are single-phase processes while the evaporation lies in a two-phase region. Similarly, the working fluid in the condenser goes through two-phase condensation and single-phase subcooling. Therefore, the calculation of evaporation and condenser can be divided into single-phase and two-phase convective heat transfer.

2.2.1 Single-phase convective heat transfer

For single-phase convective heat transfer of plate heat exchanger, Chishom and Wanniarachchi correlations are used to calculate the Nusselt number of warm seawater, cold seawater working fluid in condenser and evaporator in single-phase region (Garcia *et al.*, 2007).

$$Nu_{\mathrm{s}} = 0.724\left(\frac{6\beta}{\pi}\right)^{0.646} Re_{\mathrm{s}}^{0.583} Pr_{\mathrm{s}}^{1/3} \tag{6}$$

where, β is the ripple angle plate, Re and Pr are Reynolds number and Prandtl number, subscript s refers to single-phase. Convective heat transfer hs is calculated by:

$$h_{\mathrm{s}} = \frac{\lambda \cdot Nu_{\mathrm{s}}}{d_{\mathrm{e}}} \tag{7}$$

2.2.2 Two-phase convective heat transfer

In both the condenser and evaporator, two-phase convective heat transfer of the working fluids is calculated by the modified LMTD method. The two-phase region is divided into multiple small sections, in which the thermal and physical properties are considered unchanged. For each section i, the Nusselt number can be calculated using Equation 8 (Wang *et al.* 2013).

$$Nu_{\mathrm{eva,t},i} = 1.926 Pr_{\mathrm{l}}^{1/3} Bo_{\mathrm{eq},i}^{0.3} Re_{\mathrm{eq},i}^{0.5}\left[1 - x_{\mathrm{m},i} + x_{\mathrm{m},i}\left(\frac{\rho_{\mathrm{l}}}{\rho_{\mathrm{s}}}\right)^{0.5}\right] \tag{8}$$

where, subscript t refer to the evaporator and two-phase flow region, Pr_l is the Prandtl number of the saturated liquid state, x_m is the vapor fraction, $Bo_{eq,i}$ and $Re_{eq,i}$ are the equivalent Boiling number and equivalent Reynolds number respectively. Therefore, for the evaporation process, the convective heat transfer coefficient $h_{eva,t}$ of each unit in two-phase region can be calculated using Equation 9.

$$h_{\mathrm{eva,t}} = \frac{\lambda_{\mathrm{l}} \cdot Nu_{\mathrm{eva,t},i}}{d_{\mathrm{e}}} \tag{9}$$

where, λ_l stands for heat conductivity of the liquid.

After the vapor exits from turbine outlet and enters condenser, it flows within the narrow channel between plates at high flow rate and is condensed by the cold seawater. For the two-phase region in the condenser, the liquid film thickness increases gradually along the flow rate direction and heat conductivity gradually decreases. The convective heat transfer coefficient for the two-phase region in the condenser can be calculated using Equation 10-11 (Yan *et al.* 1999).

$$Nu_{\mathrm{con,t}} = 4.118 Re_{eq}^{0.4} Pr_{l}^{1/3} \tag{10}$$

$$\mathrm{h}_{\mathrm{con,t}} = \frac{\lambda_{\mathrm{l}} \cdot Nu_{\mathrm{con,t}}}{d_{\mathrm{e}}} \tag{11}$$

2.3 Thermo-economic model

To evaluate the economic viability of the ocean thermal energy conversion (OTEC) system, a thermal economic model for the system is constructed, using the total investment cost and the levelized cost of energy (LCOE) as economic indicators. The Module Costing Technique (Turton *et al.*, 2018) is utilized for the cost estimation of OTEC systems, which uses the equipment procurement cost C_{P}^{0} under basic conditions (using carbon steel materials at atmospheric pressure) as the base purchase cost for equipment, and employs fitting relationships with the same form for different equipment to calculate equipment costs. The equations for the calculation are as follows:

$$\log_{10} C_{\mathrm{P,e}}^{0} = K_{1,\mathrm{e}} + K_{2,\mathrm{e}} \log_{10}(Y) + K_{3,\mathrm{e}}[\log_{10}(Y)]^2 \tag{12}$$

$$C_{\mathrm{BM,e}} = C_{\mathrm{P,e}}^{0} \cdot \left[Z_{1,\mathrm{e}} + Z_{2,\mathrm{e}} \cdot (F_{\mathrm{M,e}} F_{\mathrm{P,e}})\right] \tag{13}$$

$$C_{\mathrm{BM,tur}} = C_{\mathrm{P,tur}}^{0} \cdot F_{\mathrm{tur}} \tag{14}$$

$$\log_{10} F_{\mathrm{P,e}} = B_{1,\mathrm{e}} + B_{2,\mathrm{e}} \log_{10}(P) + B_{3,\mathrm{e}}[\log_{10}(P)]^2 \tag{15}$$

$$C_{\mathrm{OTEC}} = C_{\mathrm{BM,eva}} + C_{\mathrm{BM,con}} + C_{\mathrm{BM,pump}} + C_{\mathrm{BM,tur}} + C_{\mathrm{BM,ele}} \tag{16}$$

$$C_{\text{OTEC,2019}} = C_{\text{OTEC,2001}} \cdot \left(\frac{CEPCI_{2019}}{CEPCI_{2001}}\right) \tag{17}$$

$$LCOE = \frac{\frac{i(1+i)^n}{(1+i)^n-1} \cdot C_{OTEC,2019} + r_{\text{M}} C_{\text{OTEC,2019}}}{W_{\text{net}} \cdot t_{\text{op}}} \tag{18}$$

Here, the subscript e represent the equipment, including plate heat exchanger (PHE), turbine (Tur), pump (Pump), and generator (Gen), i is the annual interest rate selected as 5%, and n is the number of years of operation assumed to be 20 years.

Table 2 Bare model cost parameters

e	Y	K_1	K_2	K_3	Z_1	Z_2	B_1	B_2	B_3	F_M	$F_{P,e}$	F_{tur}
PHE	A/(m^2)	4.6656	-0.1557	0.1547	0.96	1.21	0	0	0	2.4	Eq.(28)	-
Tur	W/(kW)	2.2476	1.4965	-0.1618	-	-	-	-	-	-	-	3.5
Pump	W/(kW)	3.3892	0.0536	0.1538	1.89	1.35	-0.3935	0.3957	-0.00226	2.15	Eq.(28)	-
Gen	P/(kW)	$C_{\text{BM,ele}} = 1850000\left(\frac{P}{11800}\right)^{0.94}$										

2.4 Bi-objective optimization

The installed capacity and cycle thermal efficiency of the ocean thermal energy conversion (OTEC) system are chosen as the objective functions for optimization. The decision variables for optimization are the evaporator temperature (T_{eva}), condenser temperature (T_{con}), turbine inlet steam superheat (T_{sh}), and working fluid mass flow rate (m_{wf}). Under given cold and heat source conditions, the multi-objective optimization problem of the ocean thermal energy conversion system can be described as follows:

$$\begin{cases} Max\{W_{tur} = f_1(T_{\text{eva}}, T_{\text{con}}, T_{\text{sh}}, m_{\text{wf}})\} \\ Max\{\eta_{\text{thermal}} = f_2(T_{\text{eva}}, T_{\text{con}}, T_{\text{sh}}, m_{\text{wf}})\} \end{cases} \tag{19}$$

For the design of ocean thermal energy conversion (OTEC) systems, considering the potential damage to turbine blades caused by liquid droplets in the turbine, there are constraints on the dryness fraction of turbine exhaust during the thermodynamic cycle. Additionally, the heat exchange process in the heat exchangers is limited by the pinch point temperature difference (T_{pp}). Furthermore, the manufacturing cost of the OTEC system is also constrained. Therefore, the constraints for optimizing ocean thermal energy conversion systems are:

$$x_{\text{tur,out}} \geq x_{\text{tur,en}} \tag{20}$$

$$T_{\text{pp,eva}} \geq T_{\text{pp.en}} \tag{21}$$

$$T_{\text{pp,con}} \geq T_{\text{pp,en}} \tag{22}$$

$$C_{\text{OTEC,2019}} \leq C_{\text{OTEC,en}} \tag{23}$$

$x_{tur,out}$ is the dryness fraction of the exhaust at the outlet of the turbine, and to ensure the safety of the system operation, it is required to design the turbine outlet exhaust dryness fraction to be greater than or equal to 0.98. $T_{pp,eva}$ and $T_{pp,con}$ are the pinch point temperature differences of the evaporator and condenser, respectively, which are typically located at the saturated liquid point of the working fluid in the evaporator (i.e., state point 3) and the saturated gas point of the working fluid in the condenser (i.e., state point 7). Noted that the improved NSGA-II proposed by Deb *et al.* (2002) is used to solve this multi-objective problem as it offers a robust and effective approach for optimizing ORC system. Its ability to handle multiple objectives, generate Pareto-optimal solutions, maintain convergence and diversity, and efficiently explore the design space makes it a valuable tool for finding optimal designs in ORC-based ocean thermal energy conversion system. Figure 2 depicts the flowchat of the optimization process.

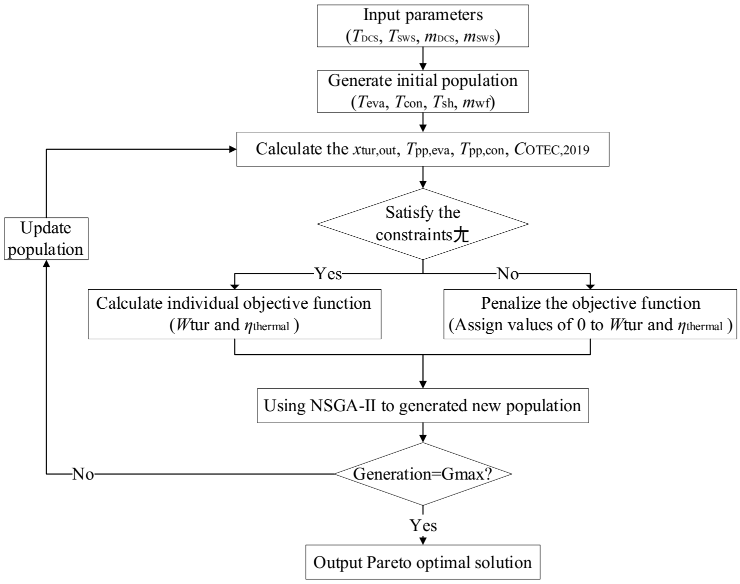

Figure 2: Optimization flowchart.

3 RESULTS AND DISCUSSION

In this section, the decision variables are set as the evaporator temperature, condenser temperature, superheat, and working fluid flow rate, with the system investment cost as a constraint. The turbine output power and cycle thermal efficiency are chosen as objective functions. Genetic algorithm is used to optimize the ocean thermal energy conversion (OTEC) power generation efficiency, and the Pareto front of the bi-objective optimization is obtained. Table 3 gives the input data of the genetic algorithm. Based on the optimization results, the performance of the OTEC system are examined for different installed capacities. 684

Table 3 Input data for genetic algorithm

Items	Values
Population size	200
Number of iterations	200
Crossover rate	0.9
Mutation rate	0.2

Figure 3 shows the Pareto front obtained with sea water mass flow rates as design parameters, where the temperature of the warm and cold seawater is fixed. It can be observed that for the same installed capacity, a larger seawater mass flow rate leads to a higher optimal thermal efficiency of the system. This is mainly because a larger seawater mass flow rate allows for higher evaporator temperature and lower condenser temperature, according to the Carnot cycle principle. Additionally, Figure 4 presents the change in generational distance with evolution generations, showing that the algorithm converges around 100 generations.

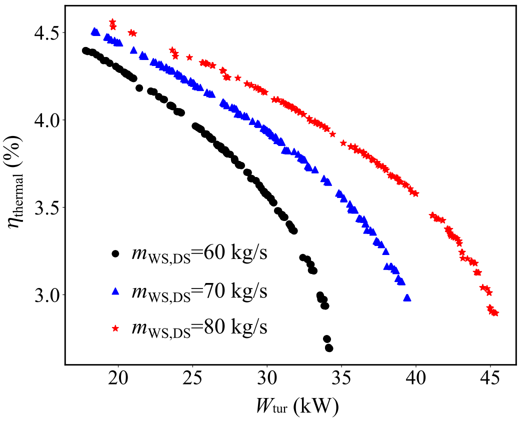

Figure 3: Pareto frontier

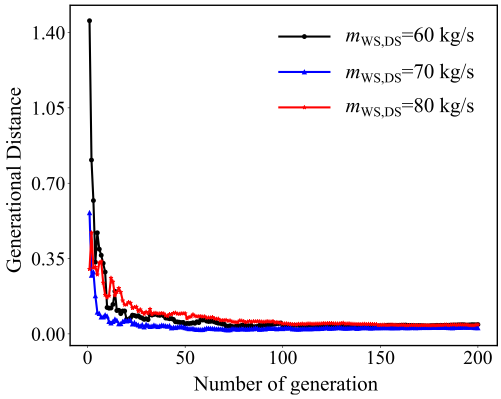

Figure 4: Relationship among number of generations and generation distance.

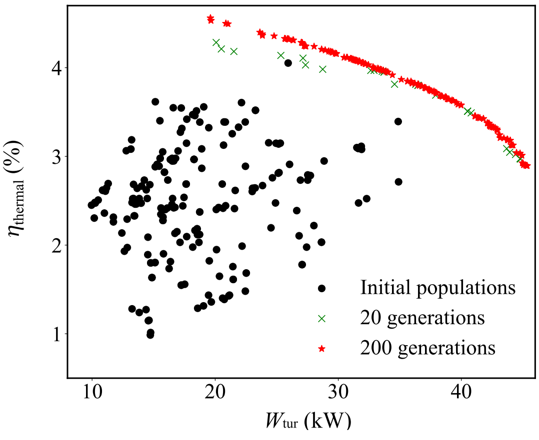

Figure 5: Non-dominated solutions of different generations and initial populations.

To quantify the optimization process and results of the OTEC system's design parameters, with seawater flow rates of hot and cold sides set at 80 kg/s as the design parameters, the system design parameters were optimized. Figure 5 shows the initial population and the non-dominated solution set obtained from the 20th and 200th generations of the optimization process. Figure 6 presents the net power generation capacity, investment cost, and decision variables for some of the Pareto optimal solutions. These solutions represent a trade-off between the two objective functions, and design engineers can choose the best solution for different application conditions. In other words, each set of solutions ensures the optimal thermal efficiency of the system for a given installed capacity. The solution number in Figure 6 is sorted in ascending order of installed capacity, and from the results, it can be observed that under the given constraints, as the installed capacity increases, the optimal evaporating temperature decreases, the condensing temperature increases, the working fluid mass flow rate increases, which in turn leads to a decrease in the average heat absorption temperature and an increase in the average heat rejection temperature, resulting in lower optimal thermal efficiency, which is in accordance with the Carnot theorem. In other words, increasing the installed capacity of the system comes at the cost of sacrificing the cycle thermal efficiency under the given boundary conditions. Furthermore, as the installed capacity increases, the net output power of the system gradually increases, and the evaporator and condenser areas also increase, as well as the investment cost, but all remain within the given cost constraints.

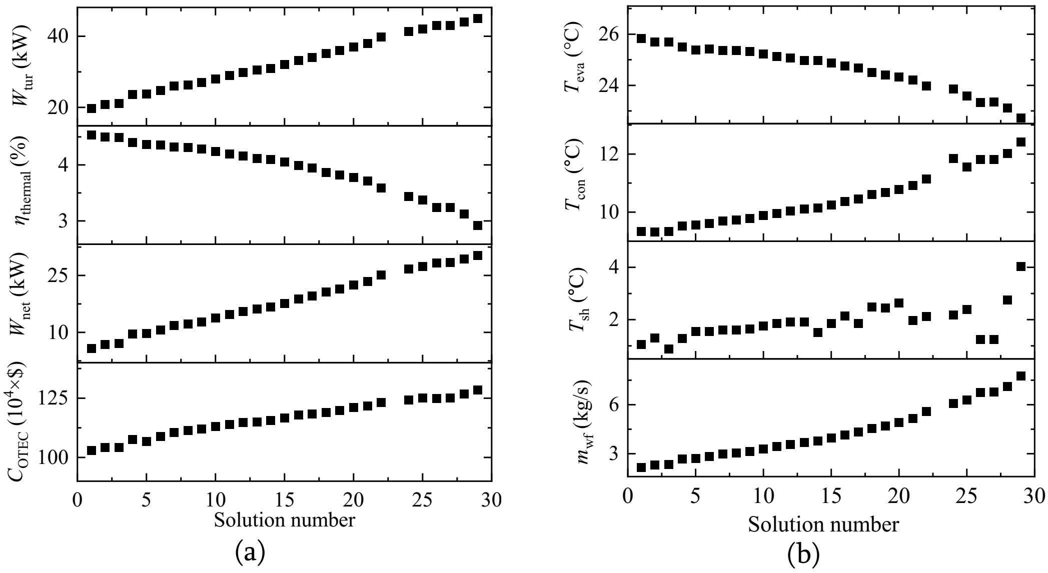

Figure 6: Optimal results of Pareto frontier: (a) objection function, (b) decision variable.

The design parameters of 20kW, 30kW, and 40kW were selected from the optimization results, and the system's other thermodynamic parameters and economic parameters are further obtained, as shown in Table 4. For the oceanic temperature difference closed-cycle power generation system with a capacity of 30kW, using R134a as the organic working fluid, the optimal evaporating temperature is 24.98°C, the condensing temperature is 10.11°C, the superheat is 1.91°C, the mass flow rate of the working fluid is 3.70 kg/s, and the net power generation capacity of the system is 16.17kW. The required evaporator and condenser areas are 122.95 m2 and 57.64 m2, respectively. The total investment cost is 1.1499 million US dollars, and the levelized cost of electricity is 0.86 US dollars/kWh.

Table 5 Performance evaluation of optimized OTEC plants

Item	Unit	20 kW-class	30 kW-class	40 kW-class
W_{tur}	kW	20	30	40
W_{net}	kW	5.70	16.17	25.13
$\eta_{thermal}$	%	4.531	4.116	3.587
T_{eva}	°C	25.83	24.98	23.98
T_{con}	°C	9.33	10.11	11.15
T_{sh}	°C	1.06	1.91	2.13

m_{wf}	kg/s	2.16	3.70	5.58
A_{eva}	m^2	103.02	122.95	135.63
A_{con}	m^2	43.33	57.64	67.46
C_{OTEC}	10^4 \$	102.93	114.99	123.11
LCOE	\$/kWh	2.18	0.86	0.59

4 CONCLUSIONS

To optimize the design parameters prior to the construction of the OTEC power plant, a bi-objective optimization is carried out for the OTEC system, where the evaporator temperature, condenser temperature, turbine inlet superheat, and working fluid mass flow rate are selected as decision variables. Under the constraint of system investment cost and with the objectives of OTEC system installed capacity and cycle thermal efficiency, the thermodynamic cycle parameters were optimized using genetic algorithm to obtain the Pareto optimal solution set. Each design in the solution set maximizes the cycle thermal efficiency for a given installed capacity of the OTEC system. The main findings can be summarized as follows:

(1) Higher evaporation or lower condensation temperatures will result in higher thermal efficiency, but the power output of the system will decrease. This is mainly due to a decrease in the amount of input heat.

(2) OTEC power plants exhibit economies of scale, with larger scale resulting in lower levelized cost of electricity.

(3) For a Rankine cycle-based OTEC system with an installed capacity of 30 kW, the optimal evaporator temperature was found to be 24.98°C, the condenser temperature was 10.11°C, the superheat was 1.91°C, and the working fluid mass flow rate was 3.70 kg/s. The net electricity generation capacity of the system was 16.17 kW, and the required evaporator and condenser areas were 122.95 m2 and 57.64 m2, respectively. The total investment cost of the system was 1.1499 million $, and the levelized cost of electricity was 0.86 $/kWh.

REFERENCES

Hung, T.C., Wang, S.K., Kuo, C.H., Pei, B.S., Tsai, K.F., 2010, A study of organic working fluids on system efficiency of an ORC using low-grade energy sources, *Energy*, vol. 35, no. 3:1403-1411.

Ganic, E.N., Wu, J., 1980, On the selection of working fluids for OTEC power plants, *Energy Convers. Manag.*, vol. 20, no. 1:9-22.

Araghi, A.H., Khiadani, M., Hooman, K., 2016, A novel vacuum discharge thermal energy combined desalination and power generation system utilizing R290/R600a, *Energy*, vol. 98, no. 1:215-224.

Yoon, J.I., Soo, C.H., Seol, S.H., Kim, H.U., Ha, S.J., Jung, S.H., Kim, H.J., Lee, H.S., 2015, Performance analysis of OTEC power cycle with a liquid-vapor ejector using R32/R152a, *Int. J. Heat Mass Transf.*, vol. 51, no. 11:1597-1605.

Sun, F., Ikegami, Y., Jia, B., Arima, H., 2012, Optimization design and exergy analysis of organic rankine cycle in ocean thermal energy conversion, *Appl. Ocean Res.*, vol. 35:38-46

Hu, Z., Wan, Y., Zhang, C., Chen, Y., 2022, Compression-assisted absorption refrigeration using ocean thermal energy. *Renew. Energ.*, vol. 186, 755-768.

García-Cascales, J. R., Vera-García, F., Corberán-Salvador, J. M., & Gonzálvez-Maciá, J., 2007, Assessment of boiling and condensation heat transfer correlations in the modelling of plate heat exchangers, *Int. J. Refrig.*, vol. 30 no. 6:1029-1041.

Wang, J., Yan, Z., Wang, M., Li, M., Dai, Y., 2013. Multi-objective optimization of an organic Rankine cycle (ORC) for low grade waste heat recovery using evolutionary algorithm, *Energy Convers. Manag.*, vol. 71:146-158.

Yan, Y. Y., Lio, H. C., Lin, T. F., 1999, Condensation heat transfer and pressure drop of refrigerant R-134a in a plate heat exchanger, *Int. J. Heat Mass Transf.*, vol. 42, no 6:993-1006.

Turton, R., Shaeiwitz, J., Bhattacharyya, D., Whiting, W., 2018, *Analysis, Synthesis and Design of Chemical Processes*, Pearson, New Jersey, 1520 p.
Deb, K., Pratap, A., Agarwal, S., Meyarivan, T.A.M.T., 2022. A fast and elitist multiobjective genetic algorithm: NSGA-II, *IEEE transactions on evolutionary computation*, vol. 6, no. 2:182-197.

ACKNOWLEDGEMENT

This work was supported by the National Key R&D Program of China (2019YFB1504303).

This book contains the compilation of works contributed to the *7th International Seminar on Organic Rankine Cycle Power Systems* (ORC 2023), held in Seville between the 4th and 6th of September 2023. The event was hosted by Universidad de Sevilla on behalf of the Knowledge Centre on Organic Rankine Cycle Technology (KCORC), incorporated in The Netherlands.

The ORC conference, organized biennially, stems as the only conference that is specific to ORC technology, therefore gathering a diverse community whose affiliation spans across all the interested stakeholders, not only in this particular technology but also and in a broader context, in the energy transition. Original equipment manufacturers, professional associations, end-users, investors, policy makers, academics, scientists feel at home at ORC 2023.

The almost 100 proceedings in this book cover a wide variety of topics, from fundamentals to system integration through component design, accounting for thermodynamic performance as well as component design. In addition to this, and as a new track in 2023, works on heat pump technology were also accepted in order to raise awareness of the strong ties between both technologies, specifically in energy storage applications.

This book provides an excellent overview of the current maturity of power systems based on Organic Rankine Cycle technology for applications as diverse as geothermal and waste heat recovery in industry or downstream of other prime movers (e.g., marine applications). It is also an excellent source of information to understand the current challenges faced by the technology, stemming from a very competitive market and increasingly stringent environmental regulations.

The organizers of ORC 2023 hope that the reader finds this work as exciting as the attendees to the conference and, maybe, make the decision to join the 8th edition to the conference in 2025.

KCORC
KNOWLEDGE CENTER
ORGANIC RANKINE CYCLE

eUS EDITORIAL
UNIVERSIDAD DE SEVILLA